



ELSEVIER

Contents lists available at ScienceDirect

Signal Processing: *Image Communication*journal homepage: [www.elsevier.com/locate/image](http://www.elsevier.com/locate/image)

## Fast intra-encoding algorithm for High Efficiency Video Coding

Liang Zhao<sup>a</sup>, Xiaopeng Fan<sup>a,\*</sup>, Siwei Ma<sup>b</sup>, Debin Zhao<sup>a</sup><sup>a</sup> Department of Computer Science and Technology, Harbin Institute of Technology, Harbin 150001, China<sup>b</sup> Institute of Digital Media, Peking University, Beijing 100871, China

## ARTICLE INFO

## Article history:

Received 21 February 2014

Received in revised form

16 June 2014

Accepted 16 June 2014

Available online 21 June 2014

## Keywords:

Video coding

HEVC

Fast intra-encoding

Early termination

Intra-prediction mode decision

## ABSTRACT

The emerging High Efficiency Video Coding (HEVC) standard provides equivalent subjective quality with about 50% bit rate reduction compared to the H.264/AVC High profile. However, the improvement of coding efficiency is obtained at the expense of increased computational complexity. This paper presents a fast intra-encoding algorithm for HEVC, which is composed of the following four techniques. Firstly, an early termination technique for coding unit (CU) depth decision is proposed based on the depth of neighboring CUs and the comparison results of rate distortion (RD) costs between the parent CU and part of its child CUs. Secondly, the correlation of intra-prediction modes between neighboring PUs is exploited to accelerate the intra-prediction mode decision for HEVC intra-coding and the impact of the number of mode candidates after the rough mode decision (RMD) process in HM is studied in our work. Thirdly, the TU depth range is restricted based on the probability of each TU depth and one redundant process is removed in the TU depth selection process based on the analysis of the HEVC reference software. Finally, the probability of each case for the intra-transform skip mode is studied to accelerate the intra-transform skip mode decision. Experimental results show that the proposed algorithm can provide about 50% time savings with only 0.5% BD-rate loss on average when compared to HM 11.0 for the Main profile all-intra-configuration. Parts of these techniques have been adopted into the HEVC reference software.

© 2014 Elsevier B.V. All rights reserved.

## 1. Introduction

The High Efficiency Video Coding (HEVC) standard [1] developed by the Joint Collaborative Team on Video Coding (JCT-VC) achieves equivalent subjective quality with about 50% bit rate reduction when compared to the H.264/AVC High profile [2,3]. Specifically, the bitrate decrement of HEVC intra-coding over H.264/AVC is about 25% on average [4]. HEVC adopts a similar block-based hybrid video coding framework as H.264/AVC [5,6], but provides a highly flexible hierarchy of unit representation,

which includes three units: coding unit (CU), prediction unit (PU) and transform unit (TU) [7]. CU is the basic unit used for inter/intra-coding, which allows recursive splitting into four equally sized CUs. The recursive splitting of CU is content adaptive, which is one of the biggest differences compared to H.264/AVC. PU is the basic unit used in a prediction process, whereas TU is the basic unit for transform and quantization processes. Both the sizes of PU and TU cannot exceed the size of CU.

Because of the recursive splitting, encoder needs to exhaust all combinations of all the possible sizes of CU, PU, and TU to select the optimal solution, which is very time consuming. In addition, an intra  $4 \times 4$  TU has to decide whether to skip transform or not [8].

Recently, some works on reducing the complexity of the intra-encoding process have been proposed [9–18].

\* Corresponding author.

E-mail addresses: [liang.zhao@hit.edu.cn](mailto:liang.zhao@hit.edu.cn) (L. Zhao),[fxp@hit.edu.cn](mailto:fxp@hit.edu.cn) (X. Fan), [swma@pku.edu.cn](mailto:swma@pku.edu.cn) (S. Ma),[dbzhao@hit.edu.cn](mailto:dbzhao@hit.edu.cn) (D. Zhao).

Instead of using a fixed CU depth range for each CU, a current CU depth range is adaptively determined depending on the previously encoded slices and neighboring CUs [9,10]. Meanwhile, the comparison of rate-distortion (RD) costs between the two neighboring CU depths is exploited to early terminate the splitting of CU in quad-tree structure [11]. At each CU depth, the early CU splitting and pruning methods are performed based on low-complexity RD costs and full RD costs [12]. Furthermore, a novel complexity control method by selectively constraining the depth of CU is proposed in order to not exceed a predefined complexity target for the HEVC encoder [13,14]. To reduce the complexity of intra-mode decision, a fast intra-mode decision [15] was adopted into HM1.0. It includes two steps. In the first step, all intra-prediction modes are involved in a rough mode decision (RMD) process to select the  $N$  best candidate modes in terms of the minimum sum of absolute values of Hadamard transformed coefficients and the mode bits. In the second step, the rate-distortion-optimization (RDO) process is only applied to the selected  $N$  best candidate modes. However, the correlation of the intra-prediction modes among the spatially neighboring CUs is not considered in the intra-mode decision. To further accelerate the intra-mode decision process, a fast intra-prediction mode decision exploring the correlation of intra-prediction modes between neighboring CUs is proposed [16]. To speed up the selection of the best TU depth in transform unit structure, the TU depth selection process is only applied to the best intra-prediction mode instead of all intra-prediction modes [17]. However, the statistical distribution of TU depth is not used in the TU depth selection process. For fast intra-transform skip mode decision, Francois et al. propose to disable the intra-transform skip mode for  $4 \times 4$  chroma TUs when the  $8 \times 8$  luma TU is not split into four  $4 \times 4$  TUs or none of the four  $4 \times 4$  luma TUs uses the intra-transform skip mode [18]. However, the complexity of intra-transform skip mode decision for  $4 \times 4$  luma TUs should also be reduced.

In this paper, to further relieve the computation load of the encoder, a fast intra-encoding algorithm is proposed, which is composed of four techniques. Firstly, an early termination technique for coding unit (CU) depth decision is proposed based on the depth of neighboring CUs and the comparison results of rate distortion (RD) costs between the parent CU and part of its child CUs. Secondly, the correlation of intra-prediction modes between neighboring PUs is exploited to accelerate the intra-prediction mode decision for HEVC intra-coding and the impact of the number of mode candidates after the rough mode decision (RMD) process in HM is studied in our work. Thirdly, the TU depth range is restricted based on the probability of each TU depth and one redundant process is removed in the TU depth selection process based on the analysis of the HM software. Finally, the probability of each case for the intra-transform skip mode is studied to accelerate the intra-transform skip mode decision.

The rest of this paper is organized as follows. Section 2 presents an overview of intra-encoding in HEVC. Section 3 gives a detailed description of the proposed fast intra-encoding algorithm. Experimental results are provided in Section 4. Section 5 concludes this paper.

## 2. Overview of intra-encoding in HEVC

This section reviews the intra-encoding process of HEVC from the following four aspects: coding tree unit (CTU) and coding unit (CU) structure, intra-prediction, transform unit structure, and intra-transform skip mode.

### 2.1. Coding tree unit and coding unit structure

A picture is composed of a sequence of coding tree units (CTUs). The CTU concept is similar to the macroblock in H.264/AVC [5]. The coding unit (CU) is the basic unit used for inter/intra-coding, which is the leaf node of the CTU. The largest coding unit and the smallest coding unit in a CTU is specified by  $64 \times 64$  and  $8 \times 8$  in the Main profile respectively. One example of recursive splitting for CTU is illustrated in Fig. 1.

### 2.2. Intra-prediction

As shown in Fig. 2, for intra-coded CU, there are two partition types of prediction unit (PU): Part\_2N  $\times$  2N and Part\_N  $\times$  N, where the CU size is equal to 2N  $\times$  2N and the partition type Part\_N  $\times$  N is only allowed for the smallest CU. The size of PU ranges from  $4 \times 4$  to  $64 \times 64$  and each PU has 35 intra-prediction modes, where intra-prediction mode 0 refers to the planar intra-prediction, mode 1 to DC prediction, and modes 2–34 to angular prediction modes with angles of  $+/- [0, 2, 5, 9, 13, 17, 21, 26, 32]/32$  [4]. Fig. 3 further illustrates the 35 intra-prediction modes. When compared to the 9 intra-prediction modes in H.264/AVC, the 35 intra-prediction modes in HEVC are more adequate to model accurately different directional structures as well as homogeneous regions with gradually changing sample values. The number of intra-prediction

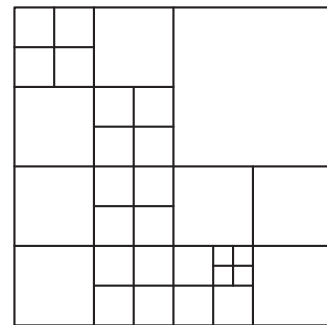


Fig. 1. Example of CTU structure.

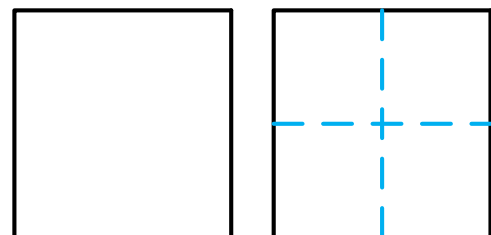


Fig. 2. Part\_2N  $\times$  2N (left) and Part\_N  $\times$  N (right).

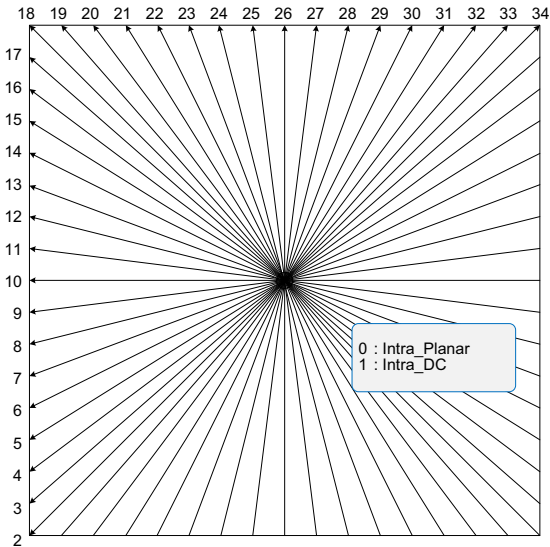


Fig. 3. Intra-prediction modes in HEVC.

modes is selected to make a good tradeoff between encoding complexity and coding efficiency for typical video [4].

### 2.3. Transform unit structure

The transform unit (TU) is the basic unit used for the transform and quantization processes. The sizes of TU range from  $4 \times 4$  to  $32 \times 32$ . For intra-coded CU, the size of TU cannot exceed the size of PU, because the residuals of neighboring PUs should be reconstructed before the intra-prediction of current PU. In one CU, HEVC allows the residual block to be split into multiple TUs. The multiple TUs in one CU are arranged in a quad-tree structure as illustrated in Fig. 4, where solid line denotes the CU boundary and dotted line denotes the TU boundary.

### 2.4. Intra-transform skip mode

Different from natural video, compound video has their own features especially on the text and graphics blocks. First, edges between letters and background in compound video are much sharper than those in natural video. Second, shapes of edges are usually complicated and hard to predict through neighboring samples. For such text and graphics blocks, traditional transform fails to give a compact representation in the transform domain. Accordingly, the intra-transform skip mode is more efficient for these blocks [19]. In HEVC, block-based intra-transform skip mode is adopted to process compound video. Except for adding one flag to indicate whether an intra- $4 \times 4$  TU uses transform skip mode or not, there is no change to the prediction, de-quantization, in-loop filters, and entropy coding. When transform skip mode is selected, transform is skipped from the coding structure. To make a tradeoff between the coding complexity and performance, intra-transform skip mode is only applied to  $4 \times 4$  TUs.

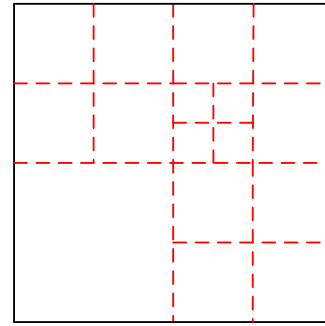


Fig. 4. Example of transform unit structure in one CU.

## 3. Fast intra-encoding algorithm

The proposed fast intra-encoding algorithm includes four techniques, which are early termination of CU encoding, fast intra-prediction mode decision, fast TU depth selection, and fast intra-transform skip mode decision. As illustrated in Fig. 5, the flowchart of the proposed fast intra-encoding algorithm for one CU is composed of 6 steps.

Step 1 and Step 2 correspond to early termination of CU encoding. Step 3 corresponds to fast intra-prediction mode decision. Step 5 corresponds to fast TU depth selection. Step 4 and Step 6 correspond to fast intra-transform skip mode decision. To be concrete, in Step 1, the search range of current CU depth is reduced based on the depth of neighboring CUs. In Step 2, we propose to skip the RDO process of current child CU and subsequent child CUs if the sum of RD cost of the already processed child CUs is larger than the RD cost of their parent CU. In Step 3, fast intra-prediction mode decision is employed to reduce the candidate modes selected from RMD. In Step 4, for each candidate prediction mode selected from RMD, fast intra-transform skip mode decision is employed to accelerate the intra-transform skip mode decision on the maximum allowed TU size of current PU. In Step 5, for the best intra-prediction mode, the TU depth range is restricted based on the probability of each TU depth and one redundant process is removed in the TU depth selection process based on the analysis of the HM software. In Step 6, for the best intra-prediction mode, the encoder calls fast intra-transform skip mode decision on all allowed TU sizes of current PU to decide whether to use the intra-transform skip mode or not.

In the following sub-sections, the four techniques of the proposed fast intra-encoding algorithm are described in detail.

### 3.1. Early termination of CU encoding

As shown in Fig. 6, CTU allows recursively splitting into four equally sized CU from depth 0 to depth 3, where CU in depth 0 is the root of CTU. For flat and homogeneous regions, the encoder prefers to encode them with a smaller CU depth; whereas for complicated and inhomogeneous regions, the encoder prefers to encode them with a larger CU depth. This flexibility of the coding tree structure

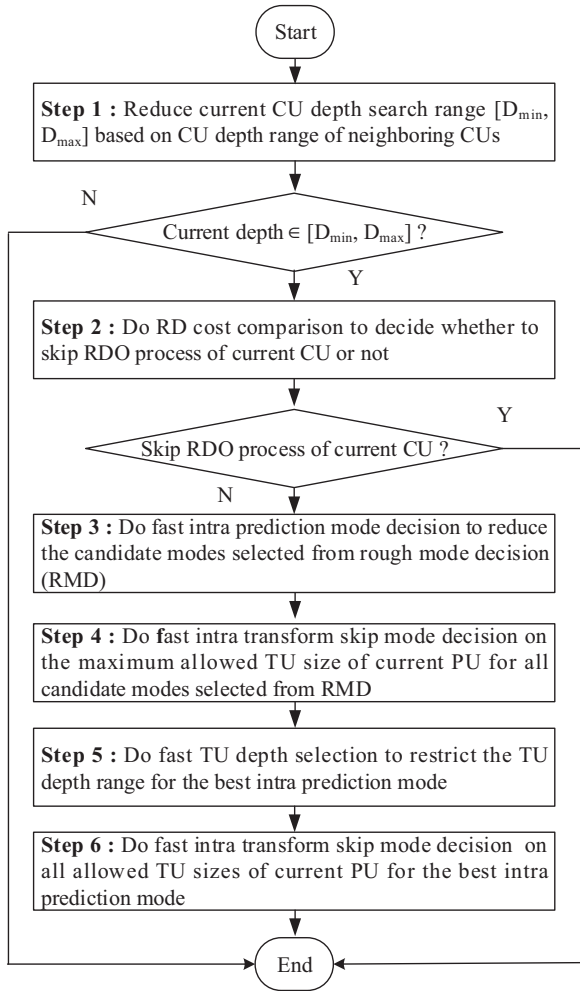


Fig. 5. Flowchart of the proposed algorithm for one CU.

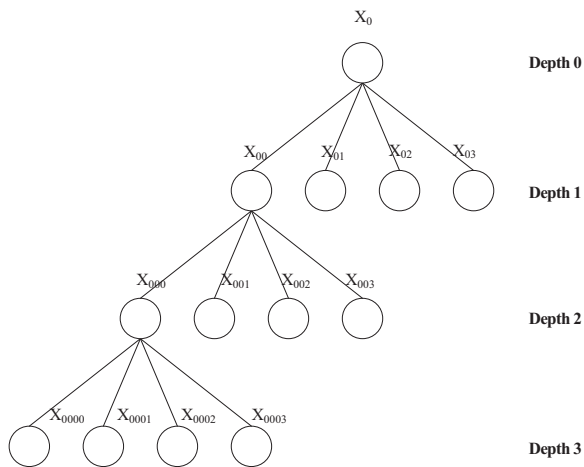


Fig. 6. Quad-tree splitting of CTU.

greatly increases the computational complexity of the encoder. Therefore, an early termination of CU encoding technique is proposed to reduce the complexity burden of the encoder, which consists of the following two steps.

In the first step, the CU level depth range selection proposed in [9] is adopted because of its effectiveness. Since neighboring CUs usually have similar CU splitting in natural images, the search range of the maximum CU depth and minimum CU depth for current CU is determined by the depth of left CU and upper CU. Denote  $D^L$ ,  $D^U$ ,  $D_{\min}^C$ ,  $D_{\max}^C$ ,  $D_{\min}^C$  and  $D_{\max}^C$  as the depth of left CU, the depth of upper CU, the minimum supported CU depth of current video sequence, the maximum supported CU depth of current video sequence, the minimum depth of current CU and the maximum depth of current CU.  $D_{\min}^C$  and  $D_{\max}^C$  are derived as follows [9]:

$$D_{\min}^C = \max(D_{\min}^C, \min(D^L, D^U) - 1) \quad (1)$$

$$D_{\max}^C = \min(D_{\max}^C, \max(D^L, D^U) + 1) \quad (2)$$

In the second step, the computation process of the remaining child CUs is proposed to be skipped when the sum of RD costs of already processed child CUs is larger than that of their parent CU. Formally, denote  $X_i$  to be the parent CU,  $F(X_i)$  to be the best RD costs of  $X_i$ ,  $X_{i,m}$  to be the child CU of  $X_i$  and  $G(X_{i,m})$  to be the best RD costs of  $X_{i,m}$ . For current  $j$ th child CU, such as  $X_{i,j}$ , if the sum of the RD costs of already processed child CUs is larger than the best RD cost of their parent CU:

$$\sum_{m=0}^{j-1} G(X_{i,m}) > F(X_i) \quad (3)$$

then the branches for  $X_{i,j}$  are skipped.

### 3.2. Fast intra-prediction mode decision

In HM11.0, the intra-prediction mode decision contains the rough mode decision (RMD) and the RDO process of intra-mode decision, where all intra-prediction modes are employed in RMD and only the selected intra-prediction modes from RMD are involved in the RDO process of intra-mode decision to compete for the best intra-prediction mode of current PU. However, the correlation of the intra-prediction modes among the spatially neighboring PUs is not considered in the intra-mode decision. In our proposed method, firstly, the correlation of intra-prediction modes between neighboring PUs is exploited to accelerate the intra-prediction mode decision; secondly, the number of mode candidates after the rough mode decision (RMD) process is reduced based on their rank.

Firstly, to characterize the correlation of the intra-prediction modes among the spatially neighboring PUs, the spatial distribution of the best intra-prediction modes in a picture is modeled as a 2-order Markov random field [20]. In this model, the probability of the optimal intra-prediction mode of current PU belonging to the set of the most probable mode (MPM) depends on the optimal modes of its neighboring encoded PUs. Formally, it is defined that

$$P(\text{MPM}_{\text{curr}} | (\text{Mode}_A, \text{Mode}_B)) \\ = P(\text{M}_{\text{curr}} \in \Gamma_{\text{MPM}} | (\text{Mode}_A = M_A, \text{Mode}_B = M_B)) \quad (4)$$

where  $\text{Mode}_A$  and  $\text{Mode}_B$  are random variables that represent the optimal modes of neighboring PUs A and B as

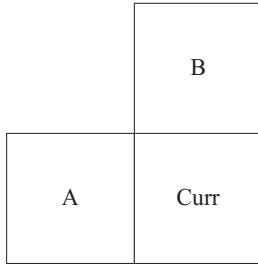


Fig. 7. Neighboring PUs of current PU.

$\Gamma_{MPM}$ derivation process:	
Input:	$M_A$ and $M_B$
Output:	$\Gamma_{MPM}$
If $M_A = M_B$	
If $M_A < 2$	$\Gamma_{MPM} = \{Planar, DC, Vertical\}$
Else	$\Gamma_{MPM} = \{M_A, 2 + ((M_A + 29) \% 32) 2 + ((M_A - 1) \% 32)\}$
Else	
If $M_A \neq Planar$ & $M_B \neq Planar$	$\Gamma_{MPM} = \{M_A, M_B, Planar\}$
Else if $M_A \neq DC$ & $M_B \neq DC$	$\Gamma_{MPM} = \{M_A, M_B, DC\}$
Else	$\Gamma_{MPM} = \{M_A, M_B, Vertical\}$
End	

Fig. 8.  $\Gamma_{MPM}$  derivation process.

Table 1

The percentages of RD optimal mode belonging to  $\Gamma_{MPM}$ .

QP	Class A (%)	Class B (%)	Class C (%)	Class D (%)	Class E (%)
22	44	42	49	55	37
27	39	36	44	49	35
32	35	32	40	44	34
37	34	30	35	39	34

depicted in Fig. 7.  $M_A$  and  $M_B$  are their possible values respectively.  $M_{curr}$  is the mode value of current PU.  $MPM_{curr}$  represents the event that RD optimal mode of current PU belongs to  $\Gamma_{MPM}$ .  $\Gamma_{MPM}$  denotes the set of MPM defined in HEVC, which has three elements. The derivation process of  $\Gamma_{MPM}$  is illustrated in Fig. 8.

Table 1 illustrates the percentages of RD optimal mode of current PU belonging to  $\Gamma_{MPM}$ , where 18 sequences in different resolutions from Class A to Class E with quantization parameters of 22, 27, 32, and 37 are taken into experiments. It can be easily seen that RD optimal mode has about 40% probability belonging to  $\Gamma_{MPM}$ . Therefore in the proposed method, every mode in  $\Gamma_{MPM}$  is always considered as the candidate mode to compete for the best intra-prediction mode.

Secondly, the number of mode candidates selected from the rough mode decision (RMD) process is reduced based on their rank. For PU sizes of  $4 \times 4$ ,  $8 \times 8$ ,  $16 \times 16$ ,

Table 2

The Percentages of the first 3,3,2,2, and 1 candidate mode to be the best prediction mode.

PU size	Class A (%)	Class B (%)	Class C (%)	Class D (%)	Class E (%)
$64 \times 64$	58	60	51	95	65
$32 \times 32$	83	81	84	86	84
$16 \times 16$	84	84	85	83	88
$8 \times 8$	87	87	87	86	91
$4 \times 4$	83	81	79	80	86

Table 3

The percentages of the combination of MPM and the first 3,3,2,2, and 1 candidate mode to be the best prediction mode.

PU size	Class A (%)	Class B (%)	Class C (%)	Class D (%)	Class E (%)
$64 \times 64$	90	93	82	95	85
$32 \times 32$	94	95	94	95	95
$16 \times 16$	94	95	94	93	96
$8 \times 8$	96	96	95	94	97
$4 \times 4$	95	94	91	91	96

$32 \times 32$ , and  $64 \times 64$ , the RMD in HM anchor selects 9, 9, 4, 4, and 5 candidate modes respectively. From the experiments, it is observed that the first 3, 3, 2, 2, and 1 candidate modes selected from the RMD can cover about 80% of the best prediction mode of current PU on average, which is illustrated in Table 2. In addition, the combination of MPM and the first 3, 3, 2, 2, and 1 candidate modes can cover about 95% of best prediction mode of current PU on average, which is further illustrated in Table 3. Therefore, in this proposed method, firstly, the number of candidates involved in the RDO process of intra-mode decision is reduced to 3, 3, 2, 2, and 1 for PU sizes of  $4 \times 4$ ,  $8 \times 8$ ,  $16 \times 16$ ,  $32 \times 32$ , and  $64 \times 64$  respectively; then all members in the set of MPM are considered as candidates in the RDO process to compete for the best intra-prediction mode. Fig. 9 shows the flowchart of fast intra-prediction mode decision, where the difference of the proposed method compared with the HM anchor is highlighted by the dotted line. In the HM anchor, the technique of our adopted proposal JCTVC-D283 is disabled, which means that only the modes selected by RMD are used to do best intra-mode decision.

### 3.3. Fast TU depth selection

In HEVC, the encoder needs to select the best TU depth to perform transform and quantization for one PU, which is very time consuming. To speed up the TU depth selection, firstly, we propose to restrict the TU depth range based on the probability of each TU depth; secondly, one redundant process is removed in the TU depth selection process based on the analysis of the HEVC reference software.

When analyzing the recursive quad-tree CU and TU structure from the whole encoding process, it is observed that the encoder prefers to select the partition with larger CU depth and smaller TU depth compared to the partition with smaller CU depth and larger TU depth. Take Fig. 10 for an example, the sum of CU depth and TU depth of the

partition in Fig. 10(a) and (b) is 4, where the CU depth of partition in Fig. 10(a) is 3, the TU depth of partition in Fig. 10(a) is 1, the CU depth of partition in Fig. 10(b) is 2 and the TU depth of partition in Fig. 10(b) is 2. When comparing these two types of partitions, the encoder prefers to select the type of partition in Fig. 10(a). To demonstrate it, 50 frames of each sequence specified in [21] are encoded with the quantization parameters of 22, 27, 32 and 37 to obtain the statistical results. As shown in Table 4, *Sum\_depth* denotes the sum of CU depth and TU depth, *C\_depth* denotes the CU depth, *T\_depth* denotes the TU depth, and *Number* denotes the number of partition with the given CU depth and TU depth. It can be seen that the *Number* of partitions with larger *C\_depth* and smaller *T\_depth* is much larger than the number of partitions with smaller *C\_depth* and larger *T\_depth* when *Sum\_depth* of two partitions is equal. Therefore, it is reasonable to reduce the TU depth for the partition with smaller CU depth.

To further demonstrate it, the probability of each TU depth for the partition with different CU depths is taken

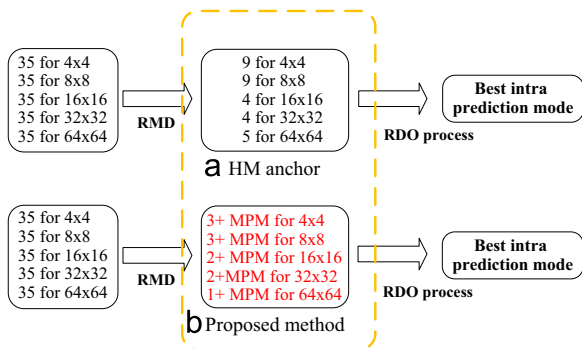


Fig. 9. This figure presents the flowchart of fast intra-prediction mode decision compared with the HM anchor.

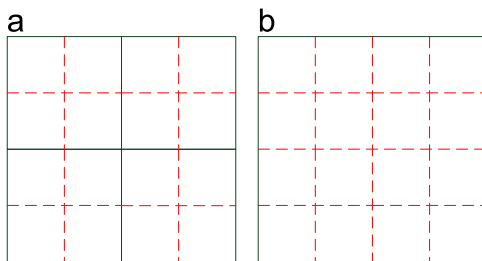


Fig. 10. Recursive CU and TU structure. The solid line denotes the CU boundary whereas the dotted line denotes the TU boundary.

into consideration. We use  $P(T\_depth = k | C\_depth = i)$  to present the probability of TU depth  $k$  for the partition with CU depth  $i$  and  $P(T\_depth \leq d | C\_depth = i)$  to present the aggregated probability of TU depth no larger than  $d$  for the partition with CU depth  $i$ . Hence, we have

$$P(T\_depth \leq d | C\_depth = i) = \sum_{k=0}^d P(T\_depth = k | C\_depth = i) \tag{5}$$

For the partition with CU depth  $i$ , the TU depth larger than  $d$  can be pruned if the following inequality holds, i.e.,  $P(T\_depth \leq d | C\_depth = i) \geq Threshold$  (6)

The *Threshold* is empirically set to 90% in our experiment. To obtain the aggregated probability of TU depth no larger than  $d$  for partition with CU depth  $i$ , 50 frames of each sequence specified in [21] are encoded with the quantization parameters of 22, 27, 32 and 37. Since the maximum supported TU size and the minimum supported TU size are  $32 \times 32$  and  $4 \times 4$  in HM common test condition respectively, the minimum TU depth for the partition with CU depth equal to 0 is 1 and the maximum TU depth for the partition with CU depth equal to 3 is 1. It is illustrated in Table 5 that for partition with CU depth equal to 0, the probability of TU depth no larger than 1 is 92%; for partition with CU depth equal to 1, the probability of TU depth no larger than 1 is 90%; for partition with CU depth equal to 2 and 3, the aggregated probability of TU depth no larger than 1 is 97% and 100% respectively. Therefore, according to Eq. (6), the allowed TU depths for partition with each CU depth in our proposed method are illustrated as follows:

$$Allowed\_Tdepth = \begin{cases} 1 & \text{if } C\_depth = 0 \\ 0 & \text{if } C\_depth = 1 \\ 0, 1 & \text{if } C\_depth = 2, 3 \end{cases} \tag{7}$$

where *Allowed\_Tdepth* denotes the allowed TU depths for partition with each CU depth.

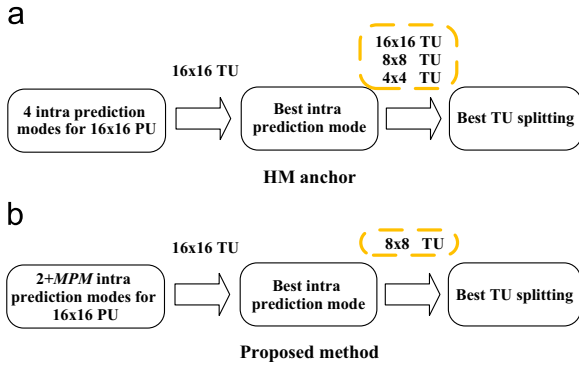
One redundant procedure is removed in the TU depth selection process. In current HM, the encoder first selects

Table 5  
The aggregated probability of TU depth no larger than 0, 1, and 2 for different CU depths.

C_depth	T_depth ≤ 0 (%)	T_depth ≤ 1 (%)	T_depth ≤ 2 (%)
0		92	100
1	90	98	100
2	83	97	100
3	63	100	

Table 4  
Number of two types of partitions for different *Sum\_depth*.

Sum_depth	Type a			Type b		
	C_depth	T_depth	Number	C_depth	T_depth	Number
2	1	1	109,953	0	2	42,856
3	2	1	738,090	1	2	129,372
4	3	1	7,823,972	2	2	927,784



**Fig. 11.** Example of the proposed TU depth selection process compared with the HM anchor.

**Table 6**  
Three cases for intra-luma and -chroma TU.

Case	Luma CU	PU	TU
Case 1	$16 \times 16$	Part_2N $\times$ 2N	$4 \times 4$
Case 2	$8 \times 8$	Part_2N $\times$ 2N	$4 \times 4$
Case 3	$8 \times 8$	Part_N $\times$ N	$4 \times 4$

the best intra-prediction mode for current PU in the intra-mode decision process as depicted in Fig. 9; then for the best intra-prediction mode, the encoder selects the best TU depth from the TU depth selection process. In the process of intra-mode decision, the encoder performs transform and quantization only on the maximum allowed TU size of current PU to compute the RD cost and select the best intra-prediction mode; whereas in the TU depth selection process, the encoder performs transform and quantization on all allowed TU sizes in the recursive TU structure to select the best TU depth. For example, as illustrated in Fig. 11, for one PU with size of  $16 \times 16$ , the encoder performs transform and quantization on TU size of  $16 \times 16$  to select the best intra-prediction mode in the intra-mode decision process. Then for the best intra-prediction mode, the encoder performs transform and quantization on TU sizes of  $16 \times 16$ ,  $8 \times 8$ , and  $4 \times 4$  to select the best TU depth. It is obvious to observe that for the best intra-prediction mode, the RD costs with TU size of  $16 \times 16$  have been computed twice in Fig. 11. Therefore, this redundant computation is proposed to be removed in the TU depth selection process to reduce the encoder complexity, which is highlighted by the dotted line. Since the maximum TU depth is proposed to set to 1 for partition with CU depth equal to 2, the RDO process of the TU size of  $4 \times 4$  is also removed from this proposed method in Fig. 11.

### 3.4. Fast intra-transform skip mode decision

In current HM, for an intra  $4 \times 4$  luma or chroma TU, regardless of the size of CU and the partition mode, the transform skip mode is used. Specifically, for intra-luma TU, there are three cases where the transform skip mode is applied, as shown in Table 6. For intra-chroma TU, besides

**Table 7**  
The fourth case for intra-chroma TU.

Case	Luma CU	PU	TU
Case 4	$32 \times 32$	Part_2N $\times$ 2N	$4 \times 4$

**Table 8**  
The number of transform skip modes in different cases for intra-luma TU

Sequence	Case 1	Case 2	Case 3
<i>BasketballDrillText</i>	1586	4078	20,741
<i>ChinaSpeed</i>	3528	14,439	161,267
<i>SlideEditing</i>	5434	20,573	305,036
<i>SlideShow</i>	517	2232	21,022

**Table 9**  
The number of transform skip modes in different cases for intra-chroma TU.

Sequence	Case 1	Case 2	Case 3	Case 4
<i>BasketballDrillText</i>	181	1346	6671	0
<i>ChinaSpeed</i>	910	3886	36,268	0
<i>SlideEditing</i>	1709	8526	132,938	0
<i>SlideShow</i>	83	324	2364	0

the above three cases, there is one additional case as shown in Table 7.

To analyze the effectiveness of intra-transform skip mode in different cases, four compound sequences provided by [21] are employed to perform experiments. They are *BasketballDrillText*, *ChinaSpeed*, *SlideEditing*, and *SlideShow* respectively. Tables 8 and 9 show the number of selected transform skip modes for intra-luma and -chroma TU in different cases. It is shown that most of the selected transform skip modes appear in the third case both for intra-luma and -chroma TU. Therefore, in our proposed method, for intra-luma and -chroma TU, the transform skip mode is searched only when the third case is satisfied.

## 4. Experimental results

In order to evaluate the performance of the proposed algorithm, it is implemented into the HEVC reference software (HM11.0). Since the proposed algorithm focuses on intra-coding, experiments are carried out with Main profile all-intra-configuration. According to the specifications provided by [21], the 19 test sequences with  $2560 \times 1600$ ,  $1920 \times 1080$ ,  $1280 \times 720$ ,  $832 \times 480$ , and  $416 \times 240$  resolutions are used to evaluate the performance of the proposed algorithm. In the 19 test sequences, there are 16 common video sequences and 3 compound video sequences. The 3 compound videos are listed in the bottom of Tables 9 and 10, which are *BasketballDrillText*, *ChinaSpeed*, and *SlideEditing*. For each sequence, 50 frames are encoded with the quantization parameters of 22, 27, 32, and 37. The performance of the proposed algorithm is measured with BDBR (%) [22] and DT (%), where BDBR is used to represent the bitrate difference and DT is used to represent the encoding time decrement. For BDBR,

**Table 10**  
Results of the proposed algorithm compared to HM11.0.

Resolution	Sequence	BDBR (%)	DT (%)
2560 × 1600	<i>Traffic</i>	0.3	49
2560 × 1600	<i>PeopleOnStreet</i>	0.4	50
1920 × 1080	<i>ParkScene</i>	0.2	50
1920 × 1080	<i>Cactus</i>	0.4	51
1920 × 1080	<i>BasketballDrive</i>	0.2	51
1920 × 1080	<i>BQTerrace</i>	0.4	53
1280 × 720	<i>Vidyo1</i>	0.3	49
1280 × 720	<i>Vidyo3</i>	0.5	48
832 × 480	<i>BasketballDrill</i>	0.5	47
832 × 480	<i>BQMall</i>	0.5	49
832 × 480	<i>PartyScene</i>	0.5	50
832 × 480	<i>RaceHorses</i>	0.3	48
416 × 240	<i>BasketballPass</i>	0.5	48
416 × 240	<i>BQSquare</i>	0.5	52
416 × 240	<i>BlowingBubbles</i>	0.4	49
416 × 240	<i>RaceHorses</i>	0.4	49
832 × 480	<i>BasketballDrillText</i>	0.5	48
1024 × 768	<i>ChinaSpeed</i>	1.4	52
1280 × 720	<i>SlideEditing</i>	1.3	54
	Average	0.5	50

**Table 11**  
Results of early termination of CU encoding compared to HM11.0.

Resolution	Sequence	BDBR (%)	DT (%)
2560 × 1600	<i>Traffic</i>	0.1	14
2560 × 1600	<i>PeopleOnStreet</i>	0.1	12
1920 × 1080	<i>ParkScene</i>	0.1	12
1920 × 1080	<i>Cactus</i>	0.1	13
1920 × 1080	<i>BasketballDrive</i>	0.1	14
1920 × 1080	<i>BQTerrace</i>	0.1	18
1280 × 720	<i>Vidyo1</i>	0.1	15
1280 × 720	<i>Vidyo3</i>	0.1	16
832 × 480	<i>BasketballDrill</i>	0.1	14
832 × 480	<i>BQMall</i>	0.1	17
832 × 480	<i>PartyScene</i>	0.0	19
832 × 480	<i>RaceHorses</i>	0.1	13
416 × 240	<i>BasketballPass</i>	0.1	10
416 × 240	<i>BQSquare</i>	0.0	12
416 × 240	<i>BlowingBubbles</i>	0.0	12
416 × 240	<i>RaceHorses</i>	0.0	10
832 × 480	<i>BasketballDrillText</i>	0.1	13
1024 × 768	<i>ChinaSpeed</i>	0.0	19
1280 × 720	<i>SlideEditing</i>	0.0	22
	Average	0.1	14

positive values indicate bitrate increments whereas negative values indicate bitrate decrements. The proposed algorithm is compared to the HEVC reference software (HM11.0), and fast CU size decision and mode decision algorithm (FCSMD) [10]. Because the proposed fast intra-prediction mode decision and the fast intra-transform skip mode decision have been adopted into the HEVC reference software [23,24], these two techniques are disabled in the software of HM11.0 and FCSMD. More specifically, the flag TransformSkipFast is set equal to 0 in the configuration file and the macro symbol FAST\_UDI\_USE\_MPM is set to 0 in the reference software.

Table 10 shows the performance of the proposed algorithm compared to HM11.0. The proposed algorithm can reduce the encoding time about 50% on average for all

sequences. The maximum reduction of encoding time is 54% in *SlideEditing* (1280 × 720) whereas the minimum reduction of encoding time is 47% in *BasketballDrill* (832 × 480). Because unnecessary CU sizes, intra-prediction modes and TU sizes are not included in the RDO process, the encoding time reduction is high. On the other hand, the bitrate increase is negligible in Table 10, where the average bitrate increase is just 0.5% and the maximum bitrate increase is 1.3%. As shown in Table 11, early termination of CU encoding achieves 14% encoding time reduction with about 0.1% BD-rate loss on average for all sequences when compared to HM11.0. The maximum reduction of encoding time is 22% for *SlideEditing* (1280 × 720) whereas the minimum reduction of encoding

**Table 12**  
Results of fast intra-prediction mode decision compared to HM11.0.

Resolution	Sequence	BDBR (%)	DT (%)
2560 × 1600	<i>Traffic</i>	0.1	23
2560 × 1600	<i>PeopleOnStreet</i>	0.2	22
1920 × 1080	<i>ParkScene</i>	0.0	23
1920 × 1080	<i>Cactus</i>	0.1	23
1920 × 1080	<i>BasketballDrive</i>	−0.1	24
1920 × 1080	<i>BQTerrace</i>	0.1	25
1280 × 720	<i>Vidyo1</i>	0.3	19
1280 × 720	<i>Vidyo3</i>	0.3	17
832 × 480	<i>BasketballDrill</i>	−0.1	23
832 × 480	<i>BQMall</i>	0.1	24
832 × 480	<i>PartyScene</i>	0.1	21
832 × 480	<i>RaceHorses</i>	0.2	21
416 × 240	<i>BasketballPass</i>	0.5	23
416 × 240	<i>BQSquare</i>	0.1	23
416 × 240	<i>BlowingBubbles</i>	0.1	23
416 × 240	<i>RaceHorses</i>	0.4	23
832 × 480	<i>BasketballDrillText</i>	0.1	22
1024 × 768	<i>ChinaSpeed</i>	0.7	23
1280 × 720	<i>SlideEditing</i>	0.8	26
	Average	0.2	23

**Table 13**  
Results of fast TU depth selection compared to HM11.0.

Resolution	Sequence	BDBR (%)	DT (%)
2560 × 1600	<i>Traffic</i>	0.2	13
2560 × 1600	<i>PeopleOnStreet</i>	0.2	14
1920 × 1080	<i>ParkScene</i>	0.1	15
1920 × 1080	<i>Cactus</i>	0.2	15
1920 × 1080	<i>BasketballDrive</i>	0.2	14
1920 × 1080	<i>BQTerrace</i>	0.2	13
1280 × 720	<i>Vidyo1</i>	0.3	11
1280 × 720	<i>Vidyo3</i>	0.2	14
832 × 480	<i>BasketballDrill</i>	0.2	15
832 × 480	<i>BQMall</i>	0.2	16
832 × 480	<i>PartyScene</i>	0.1	17
832 × 480	<i>RaceHorses</i>	0.1	15
416 × 240	<i>BasketballPass</i>	0.2	15
416 × 240	<i>BQSquare</i>	0.1	17
416 × 240	<i>BlowingBubbles</i>	0.0	15
416 × 240	<i>RaceHorses</i>	0.1	15
832 × 480	<i>BasketballDrillText</i>	0.2	14
1024 × 768	<i>ChinaSpeed</i>	0.2	13
1280 × 720	<i>SlideEditing</i>	0.2	9
	Average	0.2	14

time is 10% for *BasketballPass* (416 × 240). As shown in Table 12, fast intra-prediction mode decision achieves 23% encoding time reduction with about 0.2% BD-rate loss on average for all sequences when compared to HM11.0. The maximum reduction of encoding time is 26% for *SlideEditing* (1280 × 720) whereas the minimum reduction of encoding time is 17% for *Vidyo3* (1280 × 720). As shown in Table 13, fast TU depth selection achieves 14% encoding time reduction with about 0.2% BD-rate loss on average for all sequences when compared to HM11.0. The maximum reduction of encoding time is 17% *PartyScene* (832 × 480) and *BQSquare* (416 × 240) whereas the minimum reduc-

tion of encoding time is 9% for *SlideEditing* (1280 × 720). As shown in Table 14, fast intra-transform skip mode decision achieves 8% encoding time reduction with about 0.1% BD-rate loss on average for all sequences when compared to HM11.0. The maximum reduction of encoding time is 11% for *ChinaSpeed* (1024 × 768) whereas the minimum reduction of encoding time is 6% for *Vidyo1* (1280 × 720).

Table 15 shows the performance of the proposed algorithm compared to FCSMD [10]. It is shown in Table 15 that the proposed algorithm can save the encoding time about 25% on average compared to FCSMD, with the maximum encoding time reduction of 35% in *PartyScene* (832 × 480) and *BQSquare* (416 × 240), and the minimum of 1% in *BasketballDrive* (1920 × 1080). Because FCSMD achieves higher encoding time reduction for sequences with large smooth regions like *BasketballDrive*, the proposed algorithm gains smaller encoding time reduction for these sequences. Furthermore, the proposed fast intra-encoding algorithm gets a 1.2% bitrate decrease on average compared to FCSMD.

Fig. 12 presents the time saving curves and RD curves of the proposed algorithm compared to HM11.0 with different QPs (22, 27, 32, and 37) for BQTerrace. As illustrated in Fig. 12(a), the proposed algorithm obtains negligible loss over different QPs. Meanwhile, as in Fig. 12(b), the proposed

**Table 14**  
Results of fast intra-transform skip mode decision compared to HM11.0.

Resolution	Sequence	BDBR (%)	DT (%)
2560 × 1600	<i>Traffic</i>	0.0	8
2560 × 1600	<i>PeopleOnStreet</i>	0.0	7
1920 × 1080	<i>ParkScene</i>	0.0	8
1920 × 1080	<i>Cactus</i>	0.0	8
1920 × 1080	<i>BasketballDrive</i>	0.0	7
1920 × 1080	<i>BQTerrace</i>	0.0	9
1280 × 720	<i>Vidyo1</i>	0.0	6
1280 × 720	<i>Vidyo3</i>	0.1	6
832 × 480	<i>BasketballDrill</i>	0.0	8
832 × 480	<i>BQMall</i>	0.0	10
832 × 480	<i>PartyScene</i>	0.1	10
832 × 480	<i>RaceHorses</i>	0.0	9
416 × 240	<i>BasketballPass</i>	0.0	10
416 × 240	<i>BQSquare</i>	0.0	7
416 × 240	<i>BlowingBubbles</i>	0.0	10
416 × 240	<i>RaceHorses</i>	0.0	9
832 × 480	<i>BasketballDrillText</i>	0.1	8
1024 × 768	<i>ChinaSpeed</i>	0.5	11
1280 × 720	<i>SlideEditing</i>	0.4	9
	Average	0.1	8

**Table 15**  
Results of the proposed algorithm compared to FCSMD.

Resolution	Sequence	BDBR (%)	DT (%)
2560 × 1600	<i>Traffic</i>	-1.2	17
2560 × 1600	<i>PeopleOnStreet</i>	-1.1	24
1920 × 1080	<i>ParkScene</i>	-1.3	17
1920 × 1080	<i>Cactus</i>	-1.0	21
1920 × 1080	<i>BasketballDrive</i>	-2.0	1
1920 × 1080	<i>BQTerrace</i>	-0.8	27
1280 × 720	<i>Vidyo1</i>	-2.4	19
1280 × 720	<i>Vidyo3</i>	-1.3	15
832 × 480	<i>BasketballDrill</i>	-0.7	30
832 × 480	<i>BQMall</i>	-1.0	31
832 × 480	<i>PartyScene</i>	-0.6	35
832 × 480	<i>RaceHorses</i>	-0.6	27
416 × 240	<i>BasketballPass</i>	-1.2	25
416 × 240	<i>BQSquare</i>	-0.7	35
416 × 240	<i>BlowingBubbles</i>	-0.8	33
416 × 240	<i>RaceHorses</i>	-0.7	33
832 × 480	<i>BasketballDrillText</i>	-0.7	32
1024 × 768	<i>ChinaSpeed</i>	-2.1	28
1280 × 720	<i>SlideEditing</i>	-2.3	34
	Average	-1.2	25

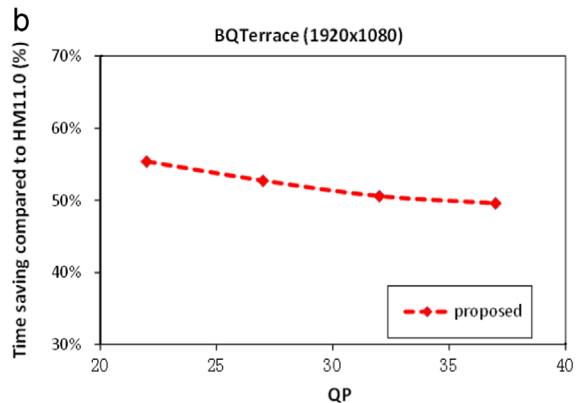
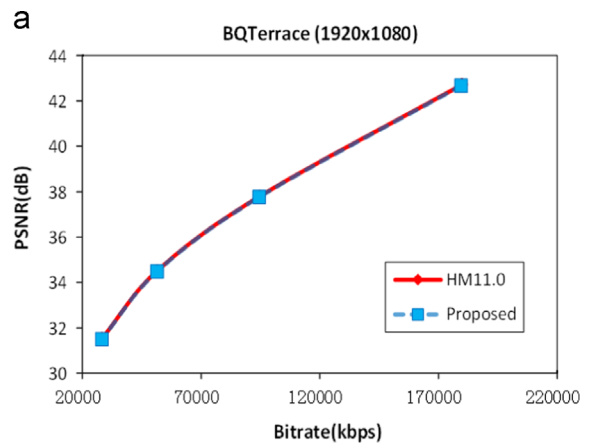


**Fig. 12.** Experimental results of BQTerrace under different QPs. (a) RD curves of “BQTerrace” and (b) Time saving curves of “BQTerrace” compared to HM11.0.

algorithm consistently achieves about 50% time savings for different QPs.

## 5. Conclusions

To alleviate the computational burden of HEVC encoder, this paper proposes a fast intra-encoding algorithm to accelerate the RDO process. The proposed fast intra-encoding algorithm consists of four novel techniques, which aim to optimize the encoder by reducing the computational intensive processing in CU depth selection, intra-prediction mode decision, TU depth selection and intra-transform skip mode decision respectively. Experimental results demonstrate that the proposed algorithm provides about 50% time savings for Main profile all-intra-configuration with only 0.5% BD-rate loss on average when compared to HM 11.0.

## Acknowledgment

This work was supported in part by the National Science Foundation of China (NSFC) under Grant nos. 61272386 and 61390513, the Program for New Century Excellent Talents in University (NCET) of China (NCET-11-0797), and the Fundamental Research Funds for the Central Universities (Grant no. HIT.BRETI.III.201221).

## References

- [1] G.J. Sullivan, J. Ohm, W.-J. Han, T. Wiegand, Overview of the high efficiency video coding (HEVC) standard, *IEEE Trans. Circuits Syst. Video Technol.* 22 (12) (2012) 1649–1668.
- [2] J. Vanne, M. Viitanen, T.D. Hamalainen, A. Hallapuro, Comparative rate-distortion-complexity analysis of HEVC and AVC video codecs, *IEEE Trans. Circuits Syst. Video Technol.* 22 (12) (2012) 1885–1898.
- [3] J. Ohm, G.J. Sullivan, H. Schwarz, T.K. Tan, T. Wiegand, Comparison of the coding efficiency of video coding standards including high efficiency video coding (HEVC), *IEEE Trans. Circuits Syst. Video Technol.* 22 (12) (2012) 1669–1684.
- [4] J. Lainema, F. Bossen, W.-J. Han, J. Min, K. Ugur, Intra coding of the HEVC standard, *IEEE Trans. Circuits Syst. Video Technol.* 22 (12) (2012) 1792–1801.
- [5] T. Wiegand, G.J. Sullivan, G. Bjontegaard, A. Luthra, Overview of the H.264/AVC video coding standard, *IEEE Trans. Circuits Syst. Video Technol.* 13 (7) (2003) 560–576.
- [6] I. Rec, H.264 & ISO/IEC 14496-10 AVC, Advanced Video Coding for Generic Audiovisual Services, May 2003.
- [7] I.-K. Kim, J. Min, T. Lee, W.-J. Han, J. Park, Block partitioning structure in the HEVC standard, *IEEE Trans. Circuits Syst. Video Technol.* 22 (12) (2012) 1697–1706.
- [8] C. Lan, J. Xu, G. Sullivan, F. Wu, Intra transform skipping, in: Joint Collaborative Team on Video Coding (JCT-VC) of ITU-T SG16 WP3 and ISO/IEC JTC1/SC29/WG11 Document JCTVC-I0408, 9th Meeting, Geneva, CH, April 2012.
- [9] X. Li, J. An, X. Guo, S. Lei, Adaptive CU depth range, in: Joint Collaborative Team on Video Coding (JCT-VC) of ITU-T SG16 WP3 and ISO/IEC JTC1/SC29/WG11 Document JCTVC-E090, Geneva, CH, March 2011.
- [10] L. Shen, Z. Zhang, P. An, Fast CU size decision and mode decision algorithm for HEVC intra coding, *IEEE Trans. Consum. Electron.* 59 (1) (2013) 207–213.
- [11] H.L. Tan, F. Liu, Y.H. Tan, C. Yeo, On fast coding tree block and mode decision for high-efficiency video coding (HEVC), in: 2012 IEEE International Conference on Acoustics, Speech and Signal Processing (ICASSP), IEEE, 2012, pp. 825–828.
- [12] S. Cho, M. Kim, Fast CU splitting and pruning for suboptimal CU partitioning in HEVC intra coding, *IEEE Trans. Circuits Syst. Video Technol.* 23 (9) (2013) 1555–1564.
- [13] G. Correa, P. Assuncao, L. Agostini, L.A. da Silva Cruz, Complexity control of high efficiency video encoders for power-constrained devices, *IEEE Trans. Consum. Electron.* 57 (4) (2011) 1866–1874.
- [14] H. Zhang, Z. Ma, Fast intra mode decision for high-efficiency video coding (HEVC), *IEEE Trans. Circuits Syst. Video Technol.* 24 (4) (2014) 660–668.
- [15] Y. Piao, J. Min, J. Chen, Encoder improvement of unified intra prediction, in: Joint Collaborative Team on Video Coding (JCT-VC) of ITU-T SG16 WP3 and ISO/IEC JTC1/SC29/WG11 Document JCTVC-C207, 3th Meeting, Guangzhou, CN, October 2010.
- [16] L. Zhao, L. Zhang, S. Ma, D. Zhao, Fast mode decision algorithm for intra prediction in HEVC, in: Visual Communications and Image Processing (VCIP), IEEE, November 2011, pp. 1–4.
- [17] B. Bross, H. Kirchner, H. Schwarz, T. Wiegand, Fast intra encoding for fixed maximum depth of transform quadtree, in: Joint Collaborative Team on Video Coding (JCT-VC) of ITU-T SG16 WP3 and ISO/IEC JTC1/SC29/WG11 Document JCTVC-C311, 3th Meeting, Guangzhou, CN, October 2010.
- [18] E. Francois, P. Onno, C. Gisquet, G. Laroche, On transform skip mode for chroma TUs, in: Joint Collaborative Team on Video Coding (JCT-VC) of ITU-T SG16 WP3 and ISO/IEC JTC1/SC29/WG11 Document JCTVC-J0171, 10th Meeting, Stockholm, SE, July 2012.
- [19] C. Lan, G. Shi, F. Wu, Compress compound images in H.264/MPGE-4 AVC by exploiting spatial correlation, *IEEE Trans. Image Process.* 19 (4) (2010) 946–957.
- [20] K. Zhang, Q. Wang, Q. Huang, D. Zhao, W. Gao, A context-based adaptive fast intra 4x4 prediction mode decision algorithm for H.264/AVC video coding, in: Picture Coding Symposium (PCS), November 2007.
- [21] F. Bossen, Common test conditions and software reference configurations, in: Joint Collaborative Team on Video Coding (JCT-VC) of ITU-T SG16 WP3 and ISO/IEC JTC1/SC29/WG11 Document JCTVC-L1100, 12th Meeting, Geneva, CH, January 2013.
- [22] G. Bjontegaard, Calculation of average PSNR difference between rd curves, in: VCEG-M33, ITU-T Q6/16, Austin, April 2001.
- [23] L. Zhao, L. Zhang, X. Zhao, S. Ma, D. Zhao, W. Gao, Further encoder improvement for intra mode decision, in: Joint Collaborative Team on Video Coding (JCT-VC) of ITU-T SG16 WP3 and ISO/IEC JTC1/SC29/WG11 Document JCTVC-D283, 4th Meeting, Daegu, KR, January 2011.
- [24] L. Zhao, J. An, Y. Huang, S. Lei, Simplification for intra transform skip mode, in: Joint Collaborative Team on Video Coding (JCT-VC) of ITU-T SG16 WP3 and ISO/IEC JTC1/SC29/WG11 Document JCTVC-J0389, 10th Meeting, Stockholm, SE, July 2012.